

Inhibition of Autotaxin Induces Imbalance of Chondrocyte Metabolism and Suppression of Autophagic Flux in Osteoarthritis

Tianqi Dai

Department of Rheumatology, The First Affiliated Hospital of Harbin Medical University

Yanli Wang

Department of Rheumatology, The First Affiliated Hospital of Harbin Medical University

Xianxu Gong

Department of Orthopaedics, The First Affiliated Hospital of Harbin Medical University

Zhiyi Zhang (✉ zhangzhiyi2014@163.com)

Department of Rheumatology, The First Affiliated Hospital of Harbin Medical University

Research Article

Keywords: Osteoarthritis, autotaxin, chondrocyte, metabolism, autophagic flux

Posted Date: April 21st, 2022

DOI: <https://doi.org/10.21203/rs.3.rs-1127455/v1>

License:  This work is licensed under a Creative Commons Attribution 4.0 International License.

[Read Full License](#)

Abstract

Background: Osteoarthritis (OA) is a degenerative joint disease that couldn't be cured by drugs. Autotaxin (ATX), which is a secretory glycoprotein related to physiological and pathological processes may possibly participate in the appropriate formation of cartilage. However, the role and specific mechanism of ATX in OA remain unclear. The present study aimed to explore the metabolism of chondrocytes and the mechanism of action of ATX in OA.

Results: In OA chondrocytes, catabolism increased and anabolism decreased. Inhibition of ATX triggered imbalanced metabolism according to the overexpression of a disintegrin and metalloproteinase with thrombospondin type 1 motif-5 (ADAMTS-5) and matrix metalloproteinase 13 (MMP13) and downregulation of collagen type II alpha 1 (COL2A1). Inhibition of ATX also caused the expression of mechanistic target of rapamycin (mTOR) declined while the expression of P62/ SQSTM1 and the microtubule-associated protein light chain 3- (LC3-) II-to-LC3-I ratio were upregulated which illustrated a blockade autophagic flux. The acidity of the lysosomes was dramatically enhanced according to LysoTracker green staining. Infection with Mcherry-EGFP-LC3 adenovirus and measurement of immunofluorescence were performed to detect the formation of autolysosomes. And it was observed that the fusion of autophagosomes and lysosomes was blocked, resulting in the obstruction of autophagic flux.

Conclusions: These data indicate that inhibition of ATX expression in chondrocytes resulted in abnormal metabolism and impaired autophagic flux via blockade of autophagosome and lysosome fusion, revealing a novel mechanism that regulated chondrocytes in OA which may provide a new target for the treatment of OA in the future.

Background

Osteoarthritis (OA) is a severe degenerative joint disease characterized by low levels of inflammation and a high degree of clinical heterogeneity resulting in a serious risk of disability [1–3]. The most common pathological change due to OA is cartilage degradation. Chondrocytes are the sole cell type in cartilage [4] and their survival depends on cartilage matrix metabolism [5].

Autotaxin (ATX) (also known as ectonucleotide pyrophosphatase/phosphodiesterase [ENPP]-2) is a 125kDa secretory glycoprotein with phosphodiesterase D activity belonging to the phosphodiesterase family which plays a critical role in both physiological and pathological processes [6]. Under physiological conditions, the ATX/LPA axis promotes cell cycle progression and enhances the proliferation of chondrocytes in zebrafish and mice [7]. Under pathological conditions, the ATX-YAP signaling axis has been shown able to mediate the participation of small extracellular vesicles from bone marrow mesenchymal stem cells (BMSCs) in the reconstruction of cartilage in the temporomandibular joint [8]. These data suggest that ATX may play a crucial role in the initiation and development of OA. However, the effects of ATX in OA or the underlying mechanism of action have rarely been reported.

The abnormal process of autophagy has proved to be closely related to OA lesions [9, 10]. Three types of autophagy are involved: macroautophagy, microautophagy, and chaperone-mediated autophagy[11]. Macroautophagy is the most common regulated form of autophagy that responds to environmental and physiological cues [12]. Autophagosomes combine with lysosomes to form autolysosomes which decompose and digest damaged molecules and organelles to maintain the activities of normal life. However, disruption of the fusion of autophagosomes and lysosomes or abnormal degradation of autolysosomes may result in impaired autophagic flux, preventing the effective decomposition and utilization of waste [13]. Here, we demonstrate that the inhibition of ATX in OA results in an imbalance in catabolism and anabolism and induces the blockade of autophagic flux caused by the impaired fusion of autophagosomes and lysosomes. The results may provide a theoretical basis for delaying or even treating OA in the future.

Results

Inhibition of ATX resulted in abnormal metabolism of chondrocytes in OA

Unbalanced cartilage matrix metabolism is an important indicator of OA. We measured and verified the expression of catabolic and anabolic proteins in normal and OA cartilage ($p < 0.05$, $n=3$) (Figure 1A-B). To explore the specific role of ATX on chondrocytes, we first determined an inhibitory concentration of inhibitor using a CCK8 assay. The results indicated that 10 μ M ATX inhibitor clearly suppressed cell survival ($p < 0.05$, $n=5$) while other concentrations had no significant effect ($p > 0.05$, $n=5$) (Figure 1C). The ATX inhibitor was then used to stimulate OA in normal chondrocytes. The results indicated that the expression of COL2A1 was significantly downregulated while MMP13 and ADAMTS-5 were upregulated after 48h ($p < 0.05$, $n=5-12$) (Figure 1D-E). This result was additionally confirmed in OA chondrocytes at the level of gene expression ($p < 0.05$, $n=5$) (Figure 1F). Thus, inhibition of ATX enhanced catabolism and reduced anabolism in human OA chondrocytes *in vitro*.

Inhibition of ATX prevented autophagic flux

To investigate the regulatory mechanism of ATX on OA chondrocytes, we observed its effect on OA autophagy by inhibition of the expression of ATX. The results of Western blotting indicated that the expression of mTOR was downregulated, while P62 and LC3-II were both upregulated, in a time-dependent manner in each case ($p < 0.05$, $n=5-12$) (Figure 2A-B). Relative measurements of mRNA expression using qRT-PCR demonstrated that *mTOR* expression decreased and *p62* and *lc3* increased following ATX inhibitor treatment after 48h ($p < 0.05$, $n=5-6$) (Figure 2C). Low mTOR expression indicated that the process of autophagy had been initiated, while the accumulation of P62 and LC3-II implied that autophagic flux had been blocked.

Inhibition of ATX promoted lysosomal number and acidity in OA chondrocytes

The blockade of autophagic flux could be explained by either impaired fusion of autophagosomes with lysosomes or autolysosome degradation failure. To explore whether P62 and LC3-II accumulated after

inhibition with ATX, the expression of LAMP1 was first measured. Both mRNA and protein analysis indicated they were slightly upregulated ($p < 0.05$, $n=6-8$) (Figure 3A-C). The data indicate that inhibition of ATX increased the number of lysosomes. Optimal lysosome function requires the ability to maintain acidic pH. LysoTracker Green is a lysosomotropic dye that permits the monitoring of pH-sensitive indices of lysosomal function [14]. FACs analysis was performed to investigate the acidity of the lysosomes. After inhibition by ATX, the acidity of the lysosomes clearly increased (Figure 3D-E). These observations demonstrated that number and acidity of lysosome were both enhanced by inhibition with ATX.

Inhibition of ATX blocked autophagic flux by the obstruction of autophagosome and lysosome fusion

mCherry-EGFP-LC3 is an important tool for the measurement of autophagic flux. An mCherry-EGFP-LC3 adenovirus was used to infect OA and normal chondrocytes which were then treated with ATX inhibitor for 24h and 48h. As shown in Figure 4A and 4B, the number of red and yellow puncta were both decreased, demonstrating the production of autolysosome was decreased (Figure 4C-D). In the process of lysosomal degradation, P62 bound to the substrate is degraded by proteolytic enzymes. Therefore, the increase of P62 level is usually considered as a marker of inhibition of autophagic flux. Confocal microscopy was further utilized to identify the localization of P62 and LAMP2. The results demonstrate that, although green and red puncta increased following the addition of ATX inhibitor, they were not overlaid (Figure 5A-D). These observations suggest that the interruption to autophagic flux was due to the impairment of autophagosome and lysosome fusion

Discussion

OA is a common degenerative disease of cartilage. The methods of therapy for OA currently consist of pain relief or surgical joint replacement, which do not fundamentally treat the disease [15]. Its detailed pathogenesis remains unclear. Here, we found that inhibition of ATX caused disruption to cartilage catabolism and anabolism, and blocked autophagic flux via inhibition of the fusion of autophagosomes and lysosomes. This suggests that abnormal expression of ATX resulted in changes to cartilage and more severe joint lesions.

ATX originally isolated as an autocrine motility factor of glycoproteins and possessing the ability to stimulate cell locomotion [16, 17]. The most recent research has revealed that ATX allows fundamental human activity to be conducted and participates in homeostasis and the development of pathological conditions [18, 19]. ATX is required during the restoration of muscles by satellite cells, while ATX conditioned ablation or drug inhibition has been shown to impair muscle regeneration [20]. Recent studies have shown that the reconstruction of cartilage in OA temporomandibular joints using extracellular vesicles is mediated via the ATX-YAP signaling pathway [8]. Previous studies have also demonstrated that ATX prevents serum-deprivation-induced apoptosis in mouse fibroblasts [21]. In addition, ATX also displays multiple types of enzymatic activity, depending on the substrate [22]. When purinergic receptors bind ATP, ATX displays ATPase activity causing an opening of the gated state, including P2X7R, mediating non-inactivated K^+ efflux and Na^+ and Ca^{2+} influx, causing rapid cellular

depolarization [23]. The studies described above are consistent with our hypothesis that ATX may indirectly regulate the development of OA chondrocytes. However, few direct studies have been conducted that can establish the effect of ATX on OA chondrocytes and the specific mechanism.

In the present study, we confirmed for the first time that inhibition of ATX increased the level of catabolism in OA chondrocytes (MMP13, ADAMTS-5), and reduced anabolism (COL2A1). Although it has been confirmed that the autophagy pathway is involved in the pathogenesis of OA [10, 24], the role of ATX in such autophagy remains unclear. The current study demonstrated that ATX inhibitors cause down-regulation of mTOR expression in OA chondrocytes, suggesting that inhibition of ATX induces mTOR-dependent activation of autophagy. Nevertheless, the autophagic substrates SQSTM1/P62 and LC3- β on the autophagosomal membrane were both upregulated, exceeding our expectations. P62 is usually degraded following autophagy by lysosomal proteases, representing the most well-known target of selective autophagy [25]. P62 can be utilized as a marker for the study of autophagic flux because P62 accumulates when autophagy is inhibited, while the level of P62 decreases due to the induction of autophagy [26, 27]. These observations suggest that autophagosomes were over accumulated and autophagic flux obstructed. The reasons for this were, therefore, investigated.

There are two possible reasons for the excessive accumulation of autophagosomes. The first is that the fusion of autophagosomes and lysosomes was blocked, and the other is that the degradation of autophagosomes failed [28]. To the best of our knowledge, mCherry-GFP-LC3 adenovirus rapidly infects primary cells, allowing the measurement of the extent of autophagic flux by the conversion of staining [29]. In the present study, we found that the area of red fluorescence decreased, indicating that the number of LC3-labeled lysosomes decreased. We also utilized immunofluorescence staining to observe the co-localization of P62 and LAMP2. Together, these results indicate that autophagosomal and lysosomal fusion was obstructed.

Some problems need to be solved according to this study. Firstly, we should further verify the effect of ATX on OA in animal models. Secondly, we should further explore the specific target and interactions caused by the inhibition of ATX, resulting in the impairment of autophagic flux in OA *in vitro*. This part of the experiment requires improvement.

Conclusions

In summary, the study demonstrated that ATX plays an important role in anabolism and catabolism in OA chondrocytes, with inhibition of ATX preventing autophagic flux. The study provides the first evidence of a link between ATX and autophagy in OA chondrocytes. Therefore, targeting ATX signaling may represent a viable therapeutic strategy for OA.

Materials And Methods

Clinical specimens

Human OA articular cartilage specimens were obtained from the femoral condyles and tibial plateaus of patients undergoing total knee arthroplasty while normal articular cartilage samples were obtained from patients with irreparable articular cartilage injury at the First Affiliated Hospital of Harbin Medical University, Harbin, People's Republic of China. The research was approved by the Ethics Committee of the First Affiliated Hospital of Harbin Medical University and was performed in accordance with the Declaration of Helsinki. Written informed consent was obtained from all patients and their family members.

Chondrocyte culture

Chondrocytes were extracted from cartilage by enzymatic digestion, as described previously [30]. Small pieces of cartilage were digested in 0.25% protease (Gibco, USA) for 30 min and then with 2mg/ml collagenase (Sigma) for 24h at 37°C. Cells were seeded at a density of 1×10^5 cells/cm² then cultured in Dulbecco's Modified Eagle Medium (DMEM; Hyclone) supplemented with 10% heat-inactivated fetal bovine serum (Gibco, USA) and antibiotics (100 µg/mL streptomycin and 100 U/mL penicillin; Beyotime, People's Republic of China) at 37°C in a humidified atmosphere of 5% CO₂. Only first and second-passage cells were used to ensure a stable phenotype.

Cell Viability Assay

A Cell Counting Kit-8 (CCK8) (Dojindo, Japan) assay was used to determine cell viability following treatment with ATX inhibitor at a variety of concentrations, as described previously, with minor modifications. Chondrocytes (1×10^4 /well) were incubated in a 96-well plate for 24h. After appropriate treatment at different drug concentrations, chondrocytes were incubated with CCK-8 solution in accordance with the manufacturer's instructions for 1h at 37°C. The quantity of dye formation was measured at 450nm.

Quantitative Real-time Polymerase Chain Reaction (qRT-PCR)

Chondrocytes were treated with ATX inhibitor (10µM, Sigma, USA) for 24h or 48h prior to total RNA extraction using TRIzol reagent (Life Technologies, USA) and then reverse transcription into cDNA (Toyobo, Japan). qRT-PCR amplification was measured using SYBR Green, in accordance with standard Bio-rad protocols. The sequences of primers used in the present study are shown in Table 1.

Table 1. Sequences of Primers.

Target gene	Forward primer (5'–3')	Reverse primer (5'–3')
<i>col2a1</i>	CATGGAGACTGGCGAGACTTG	GTGGACAGCAGGCGTAGGAA
<i>mmp13</i>	CGTATTGTTTCGCGTCATGCC	GTTCCAGCCACGCATAGTCAT
<i>adamts-5</i>	GTGGTGGTGCTAGGCCGACAA	CCACATAAATCCTCCCGAGTAAACA
<i>lc3</i>	CTTCTGAGCCAGCAGTAGGG	GGCAGAGTAGGTGGGTTGGT
<i>p62</i>	ACATAGCTTGCCTAATGGCTTTTAC	CCTGCCTGCTGACAACACCTA
<i>mTOR</i>	GGCCTGGATGGCAACTACAGA	TGACTGGCCAGCAGAGTAGGAA
<i>lamp1</i>	GTTTCTTCATTCTTTACTG	TCTCTACTGTTGTAATGT
<i>β-actin</i>	AGCCTCGCCTTTGCCGA	CTGGTGCCTGGGGCG

Western blotting (WB)

Chondrocytes were lysed in cold RIPA lysis buffer and intracellular proteins separated using 12.5% sodium dodecyl sulfate-polyacrylamide gel electrophoresis (SDS-PAGE) prior to transfer to polyvinylidene difluoride membranes, as described previously [31]. Subsequently, the membranes were blocked with 5% non-fat milk and incubated with primary antibodies overnight against the following antigens: mTOR (1:1000; Cell Signaling Technology, USA), P62 (1:1000; Abcam, UK), LC3 (1:1000; Cell Signaling Technology, USA), ADAMTS-5 (1:1000; Abcam, UK), MMP-13 (1:1000; Cell Signaling Technology, USA), COL2A1 (1:1000; Abcam, UK), and LAMP1 (1:250, Abcam; UK). They were then incubated with a secondary antibody (1:15,000; LICOR, USA) for 45 min at 37°C and washed three times with tris-buffered saline with Tween 20 (TBST). Target bands were visualized using a LICOR Odyssey chemiluminometer and analyzed using ImageJ software (National Institutes of Health, USA).

Immunofluorescence assay

Primary chondrocytes were seeded on sterile glass coverslips in 24-well plates, fixed using 4% paraformaldehyde at 4°C for 20 min, then permeabilized with 0.3% Triton X-100 for 10 min prior to blocking nonspecific binding with goat serum (Boster, People's Republic of China) for 1 hour at room temperature. The chondrocytes were then incubated with primary antibodies (20 µg/mL final concentration; Abcam, UK) overnight at 4°C and then stained with fluorophore-conjugated secondary antibodies (Abcam, UK) for 30 min at 37°C. The nuclei were stained with DAPI after washing with PBS.

LysoTracker Labeling and FACS Analysis

Intracellular lysosomes were stained with LysoTracker Green (1:20,000; Cell Signaling Technology, USA) for 30 min at 37°C in the dark and then washed. The proportion of LysoTracker-positive cells was measured by flow cytometry.

Autophagic flux analysis

Chondrocytes were transfected with HBAD-mcherry-EGFP-LC3 adenovirus (Hanbio, China) in confocal plates. After 24 hours, the chondrocytes were stimulated for the subsequent 24h or 48h using ATX inhibitor. After treatment, yellow and red puncta were detected using a confocal microscope (Nikon, Japan).

Statistical analysis

Analyses were performed using GraphPad Prism Version 5.0 (GraphPad Software, Inc., La Jolla, CA, USA) or SPSS Statistics Version 19 (IBM Corporation, Armonk, NY, USA). All collected data are represented as means \pm standard error of the mean (SEM) and analyzed using a Student's t-test or by analysis of variance (ANOVA). Values of $p < 0.05$ were considered statistically significant.

Abbreviations

OA: Osteoarthritis; ATX: Autotaxin; ADAMTS-5: A disintegrin and metalloproteinase with thrombospondin type 1 motif-5; MMP13: Matrix metalloproteinase 13; COL2A1: Collagen type II alpha 1; mTOR: Mechanistic target of rapamycin; LC3: Microtubule-associated protein light chain 3; qRT-PCR: Quantitative real-time polymerase chain reaction; WB: Western blot

Declarations

Acknowledgements

This work was supported by grants from the National Natural Science Foundation of China to Tianqi Dai (Grant Number: 82001716), Scientific research and Innovation Fund of the First Affiliated Hospital of Harbin Medical University to Tianqi Dai (Grant Number: 20201318) and Health and Health Commission of Heilongjiang Province grant to Tianqi Dai (Grant Number: 2020-103).

Authors' contributions

Tianqi Dai and Zhiyi Zhang designed the experiments. Tianqi Dai, Yanli Wang and Xianxu Gong executed the experiments and analyzed data. Tianqi Dai conceived and wrote the manuscript. All authors read and approved the final manuscript.

Funding

The National Natural Science Foundation of China to Tianqi Dai (Grant Number: 82001716). Scientific research and Innovation Fund of the First Affiliated Hospital of Harbin Medical University to Tianqi Dai (Grant Number: 20201318). Health and Health Commission of Heilongjiang Province grant to Tianqi Dai (Grant Number: 2020-103).

Availability of data and materials

The datasets used and/or analysed during the current study are available from the corresponding author on reasonable request.

Ethical Approval and consent to participate

Our study was approved by the Institutional Review Board of the First Affiliated Hospital of Harbin Medical University. Written informed consent was acquired from every participant.

Consent for publication

Not Applicable.

Competing interests

The authors declare that they have no competing interests.

Authors' information

Tianqi Dai, Degrees: Doctor, E-mail: dtq19920513@163.com

Yanli Wang, Degrees: Master, E-mail: yanli_wang75@163.com

Xianxu Gong, Degrees: Master, E-mail: 294516500@qq.com

Zhiyi Zhang, Degrees: Doctor, E-mail: zhangzhiyi2014@163.com

¹ Department of Rheumatology, The First Affiliated Hospital of Harbin Medical University, Heilongjiang, Harbin, China

² Department of Orthopaedics, The First Affiliated Hospital of Harbin Medical University, Heilongjiang, Harbin, China

References

1. Zheng L, Zhang Z, Sheng P, Mobasher A. The role of metabolism in chondrocyte dysfunction and the progression of osteoarthritis. *Ageing Res Rev.* 2021; 66:101249. <http://doi.org/10.1016/j.arr.2020.101249>.
2. Choi WS, Lee G, Song WH, Koh JT, Yang J, Kwak JS, et al. The CH25H-CYP7B1-ROR α axis of cholesterol metabolism regulates osteoarthritis. *Nature.* 2019; 566(7743):254–58. <http://doi.org/10.1038/s41586-019-0920-1>.
3. Loeser RF, Goldring SR, Scanzello CR, Goldring MB. Osteoarthritis: a disease of the joint as an organ. *Arthritis Rheum.* 2012; 64(6):1697–707. <http://doi.org/10.1002/art.34453>.
4. Hwang HS, Kim HA. Chondrocyte Apoptosis in the Pathogenesis of Osteoarthritis. *Int J Mol Sci.* 2015; 16(11):26035–54. <http://doi.org/10.3390/ijms161125943>.

5. Luo P, Gao F, Niu D, Sun X, Song Q, Guo C, et al. The Role of Autophagy in Chondrocyte Metabolism and Osteoarthritis: A Comprehensive Research Review. *Biomed Res Int*. 2019; 2019:5171602. <http://doi.org/10.1155/2019/5171602>.
6. Nikitopoulou I, Oikonomou N, Karouzakis E, Sevastou I, Nikolaidou-Katsaridou N, Zhao Z, et al. Autotaxin expression from synovial fibroblasts is essential for the pathogenesis of modeled arthritis. *J Exp Med*. 2012; 209(5):925–33. <http://doi.org/10.1084/jem.20112012>.
7. Nishioka T, Arima N, Kano K, Hama K, Itai E, Yukiura H, et al. ATX-LPA1 axis contributes to proliferation of chondrocytes by regulating fibronectin assembly leading to proper cartilage formation. *Sci Rep*. 2016; 6:23433. <http://doi.org/10.1038/srep23433>.
8. Wang Y, Zhao M, Li W, Yang Y, Zhang Z, Ma R, et al. BMSC-Derived Small Extracellular Vesicles Induce Cartilage Reconstruction of Temporomandibular Joint Osteoarthritis via Autotaxin-YAP Signaling Axis. *Front Cell Dev Biol*. 2021; 9:656153. <http://doi.org/10.3389/fcell.2021.656153>.
9. Madhu V, Guntur AR, Risbud MV. Role of autophagy in intervertebral disc and cartilage function: implications in health and disease. *Matrix Biol*. 2021; 100-101:207–20. <http://doi.org/10.1016/j.matbio.2020.12.002>.
10. Yang H, Wen Y, Zhang M, Liu Q, Zhang H, Zhang J, et al. MTORC1 coordinates the autophagy and apoptosis signaling in articular chondrocytes in osteoarthritic temporomandibular joint. *Autophagy*. 2020; 16(2):271–88. <http://doi.org/10.1080/15548627.2019.1606647>.
11. Deretic V, Levine B. Autophagy balances inflammation in innate immunity. *Autophagy*. 2018; 14(2):243–51. <http://doi.org/10.1080/15548627.2017.1402992>.
12. Mizushima N, Levine B. Autophagy in Human Diseases. *N Engl J Med*. 2020; 383(16):1564–76. <http://doi.org/10.1056/NEJMra2022774>.
13. Tai H, Wang Z, Gong H, Han X, Zhou J, Wang X, et al. Autophagy impairment with lysosomal and mitochondrial dysfunction is an important characteristic of oxidative stress-induced senescence. *Autophagy*. 2017; 13(1):99–113. <http://doi.org/10.1080/15548627.2016.1247143>.
14. Hata M, Ikeda HO, Iwai S, Iida Y, Gotoh N, Asaka I, et al. Reduction of lipid accumulation rescues Bietti's crystalline dystrophy phenotypes. *Proc Natl Acad Sci U S A*. 2018; 115(15):3936–41. <http://doi.org/10.1073/pnas.1717338115>.
15. Lange T, Deckert S, Beyer F, Hahn W, Einhart N, Roessler M, et al. An individualized decision aid for physicians and patients for total knee replacement in osteoarthritis (Value-based TKR study): study protocol for a multi-center, stepped wedge, cluster randomized controlled trial. *BMC Musculoskelet Disord*. 2021; 22(1):783. <http://doi.org/10.1186/s12891-021-04546-5>.
16. Stracke ML, Krutzsch HC, Unsworth EJ, Arestad A, Cioce V, Schiffmann E, et al. Identification, purification, and partial sequence analysis of autotaxin, a novel motility-stimulating protein. *J Biol Chem*. 1992; 267(4):2524–9.
17. Stracke ML, Clair T, Liotta LA. Autotaxin, tumor motility-stimulating exophosphodiesterase. *Adv Enzyme Regul*. 1997; 37:135–44. [http://doi.org/10.1016/s0065-2571\(96\)00017-9](http://doi.org/10.1016/s0065-2571(96)00017-9).

18. Ray R, Rai V. Lysophosphatidic acid converts monocytes into macrophages in both mice and humans. *Blood*. 2017; 129(9):1177–83. <http://doi.org/10.1182/blood-2016-10-743757>.
19. Fotopoulou S, Oikonomou N, Grigorieva E, Nikitopoulou I, Paparountas T, Thanassopoulou A, et al. ATX expression and LPA signalling are vital for the development of the nervous system. *Dev Biol*. 2010; 339(2):451–64. <http://doi.org/10.1016/j.ydbio.2010.01.007>.
20. Ray R, Sinha S, Aidinis V, Rai V. Atx regulates skeletal muscle regeneration via LPAR1 and promotes hypertrophy. *Cell Rep*. 2021; 34(9):108809. <http://doi.org/10.1016/j.celrep.2021.108809>.
21. Song J, Clair T, Noh JH, Eun JW, Ryu SY, Lee SN, et al. Autotaxin (lysoPLD/NPP2) protects fibroblasts from apoptosis through its enzymatic product, lysophosphatidic acid, utilizing albumin-bound substrate. *Biochem Biophys Res Commun*. 2005; 337(3):967–75. <http://doi.org/10.1016/j.bbrc.2005.09.140>.
22. Clair T, Lee HY, Liotta LA, Stracke ML. Autotaxin is an exoenzyme possessing 5'-nucleotide phosphodiesterase/ATP pyrophosphatase and ATPase activities. *J Biol Chem*. 1997; 272(2):996–1001. <http://doi.org/10.1074/jbc.272.2.996>.
23. Li Z, Huang Z, Bai L. The P2X7 Receptor in Osteoarthritis. *Front Cell Dev Biol*. 2021; 9:628330. <http://doi.org/10.3389/fcell.2021.628330>.
24. Sun K, Luo J, Guo J, Yao X, Jing X, Guo F. The PI3K/AKT/mTOR signaling pathway in osteoarthritis: a narrative review. *Osteoarthritis Cartilage*. 2020; 28(4):400–09. <http://doi.org/10.1016/j.joca.2020.02.027>.
25. Puissant A, Fenouille N, Auberger P. When autophagy meets cancer through p62/SQSTM1. *Am J Cancer Res*. 2012; 2(4):397–413.
26. Bjorkoy G, Lamark T, Pankiv S, Overvatn A, Brech A, Johansen T. Monitoring autophagic degradation of p62/SQSTM1. *Methods Enzymol*. 2009; 452:181–97. [http://doi.org/10.1016/S0076-6879\(08\)03612-4](http://doi.org/10.1016/S0076-6879(08)03612-4).
27. Zhao L, Liu X, Xu G, Guo Y, Sun L, Zhang C, et al. Arsenic induces mTOR-dependent autophagy, whereas it impairs the autophagy-lysosome pathway and the potential role of TFEB in cultured dendritic cells. *Metallomics*. 2020; 12(8):1230–45. <http://doi.org/10.1039/d0mt00057d>.
28. Miyazaki M, Hiramoto M, Takano N, Kokuba H, Takemura J, Tokuhisa M, et al. Targeted disruption of GAK stagnates autophagic flux by disturbing lysosomal dynamics. *Int J Mol Med*. 2021; 48(4). <http://doi.org/10.3892/ijmm.2021.5028>.
29. Mauthe M, Orhon I, Rocchi C, Zhou X, Luhr M, Hijlkema KJ, et al. Chloroquine inhibits autophagic flux by decreasing autophagosome-lysosome fusion. *Autophagy*. 2018; 14(8):1435–55. <http://doi.org/10.1080/15548627.2018.1474314>.
30. Kapoor M, Mineau F, Fahmi H, Pelletier JP, Martel-Pelletier J. Glucosamine sulfate reduces prostaglandin E(2) production in osteoarthritic chondrocytes through inhibition of microsomal PGE synthase-1. *J Rheumatol*. 2012; 39(3):635–44. <http://doi.org/10.3899/jrheum.110621>.
31. Dai T, Hu Y, Lv F, Ozawa T, Sun X, Huang J, et al. Analysis of the clinical significance of DCLK1(+) colorectal cancer using novel monoclonal antibodies against DCLK1. *Onco Targets Ther*. 2018;

Figures

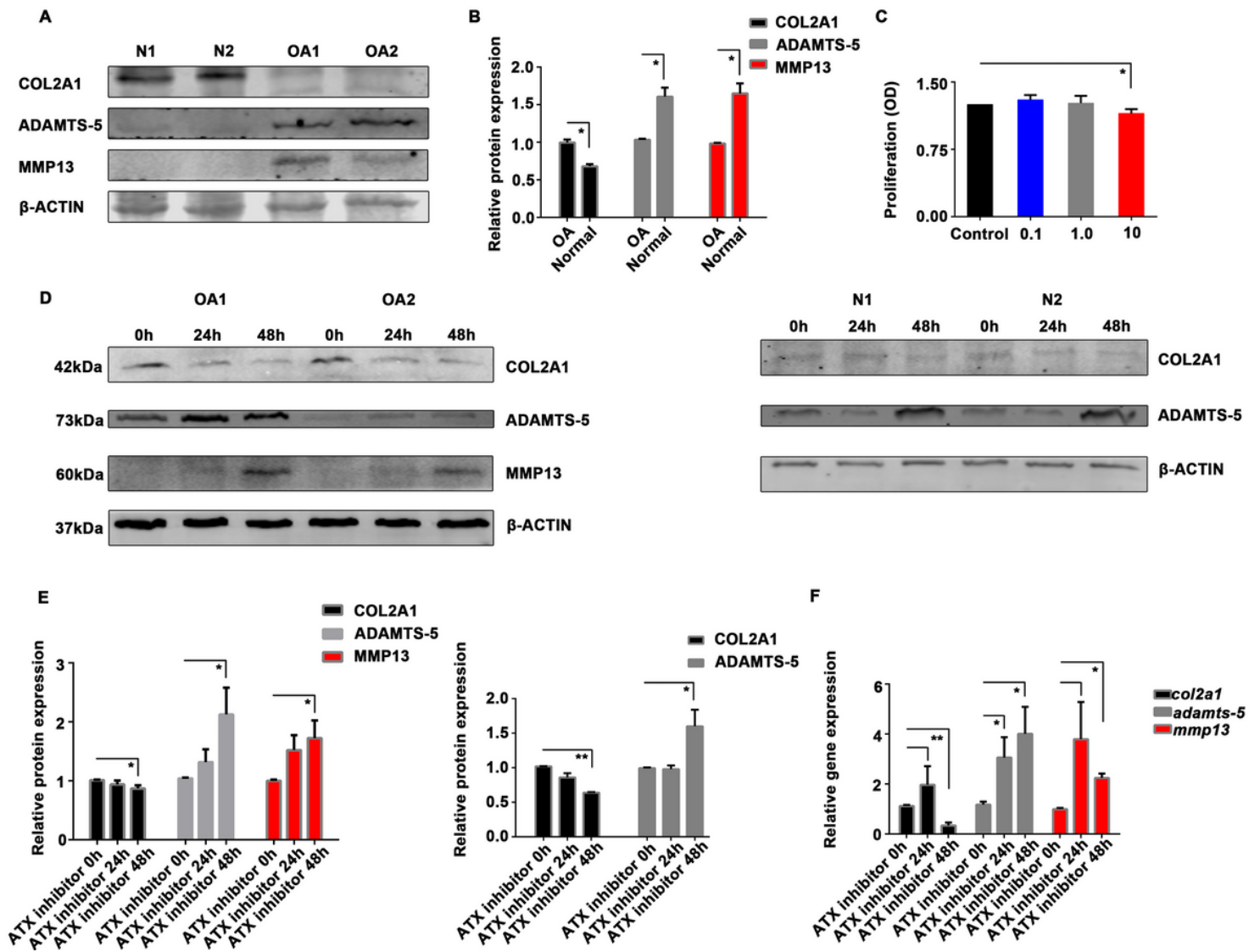


Figure 1

Inhibition of ATX caused abnormal metabolism of chondrocytes in OA. (A, B) The expression of catabolic and anabolic proteins in normal and osteoarthritis cartilage was confirmed. β -ACTIN was blotted as the loading control ($p < 0.05$, $n = 3$). The blots have been cropped. (C) CCK8 was used to measure the survival of OA chondrocytes treated with ATX inhibitors at different concentrations. There was no significant difference compared with stimulation at 0.1 or 1 μ M, but high dose (10 μ M) ATX inhibitor suppressed cell survival ($p < 0.05$, $n = 5$). (D, E) COL2A1 was downregulated and ADAMTS-5 and MMP13 upregulated when chondrocytes were treated with ATX inhibitors after 48h by Western blotting in both OA and normal chondrocytes ($p < 0.05$, $n = 5-12$). The blots have been cropped. (F) Anabolic and catabolic indices were

measured by qRT-PCR following treatment with ATX inhibitor for 24h and 48h in OA chondrocytes ($p < 0.05$, $n=5-8$). * $p < 0.05$; ** $p < 0.01$; *** $p < 0.001$; **** $p < 0.0001$

Figure 2

Inhibition of ATX prevented autophagic flux. (A, B) Measurement of the extent of autophagy using Western blot analysis in OA and normal chondrocytes. β -ACTIN was blotted as the loading control ($p < 0.05$, $n=5-12$). The blots have been cropped. (C) qRT-PCR analysis demonstrated significantly decreased mRNA expression levels of mTOR and increased expression levels of P62 and LC3 after 48h compared with at 0h ($p < 0.05$, $n=5-6$). * $p < 0.05$; ** $p < 0.01$; *** $p < 0.001$; **** $p < 0.0001$.

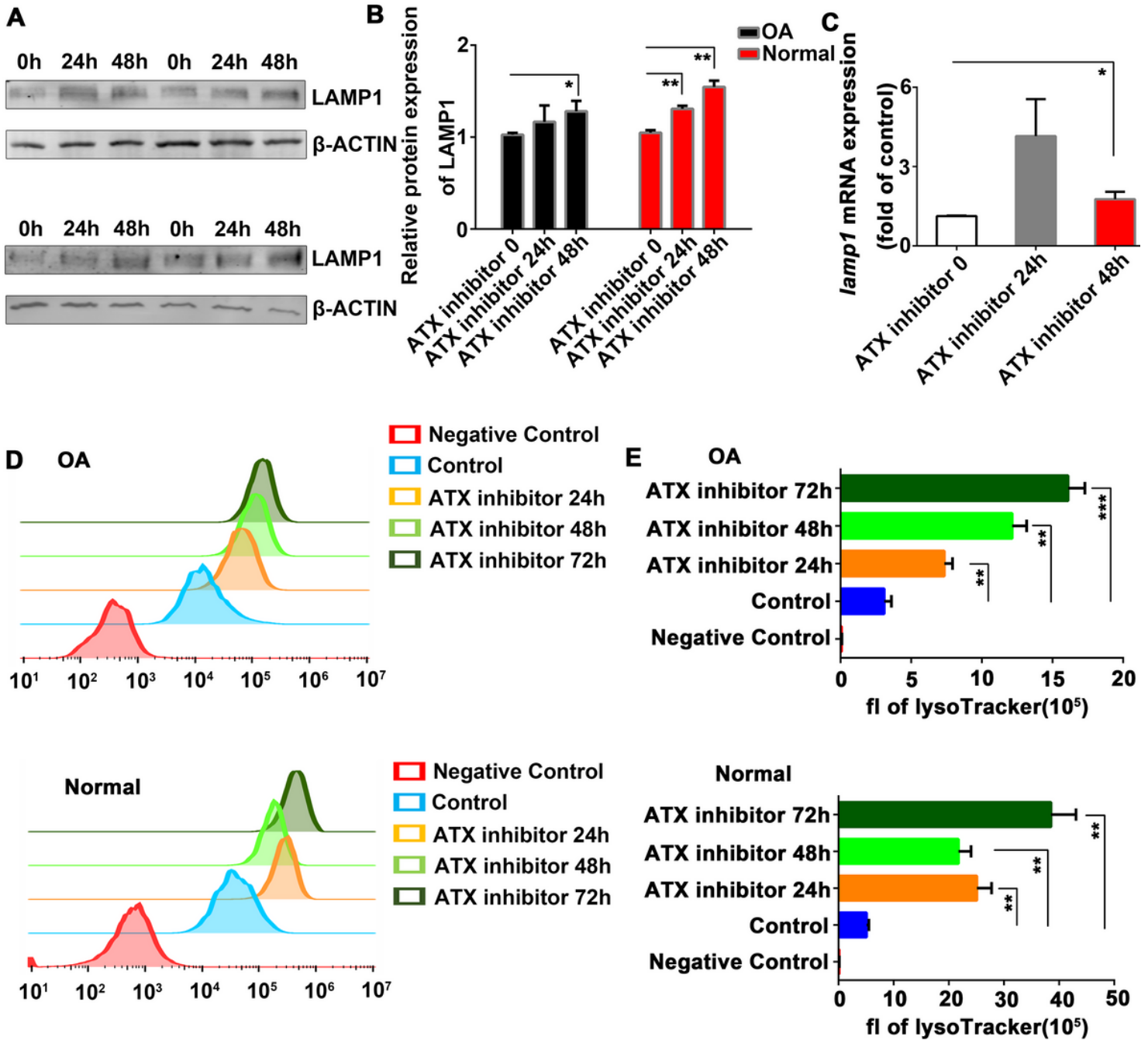


Figure 3

Inhibition of ATX promoted lysosomal function in OA chondrocytes. (A-C) Western blot and qRT PCR analyses were used to measure the expression level of LAMP1 in chondrocytes ($p < 0.05$, $n=6-8$). The blots have been cropped. (D, E) LysoTracker Green was used to measure lysosomal function using pH-sensitive indices, while FACS analysis was utilized to measure lysosomal acidity in both OA and normal chondrocytes. Lysosomal function was significantly enhanced following inhibition of ATX ($p < 0.05$, $n=3$). * $p < 0.05$; ** $p < 0.01$; *** $p < 0.001$; **** $p < 0.0001$.

Figure 4

Inhibition of ATX reduced the number of autolysosomes. (A, B) mCherry-EGFP-LC3 adenovirus was used to infect OA and normal chondrocytes. After stimulation of the cells using ATX inhibitor, the extent of red staining decreased significantly, representing decreased LC3 expression in lysosomes.

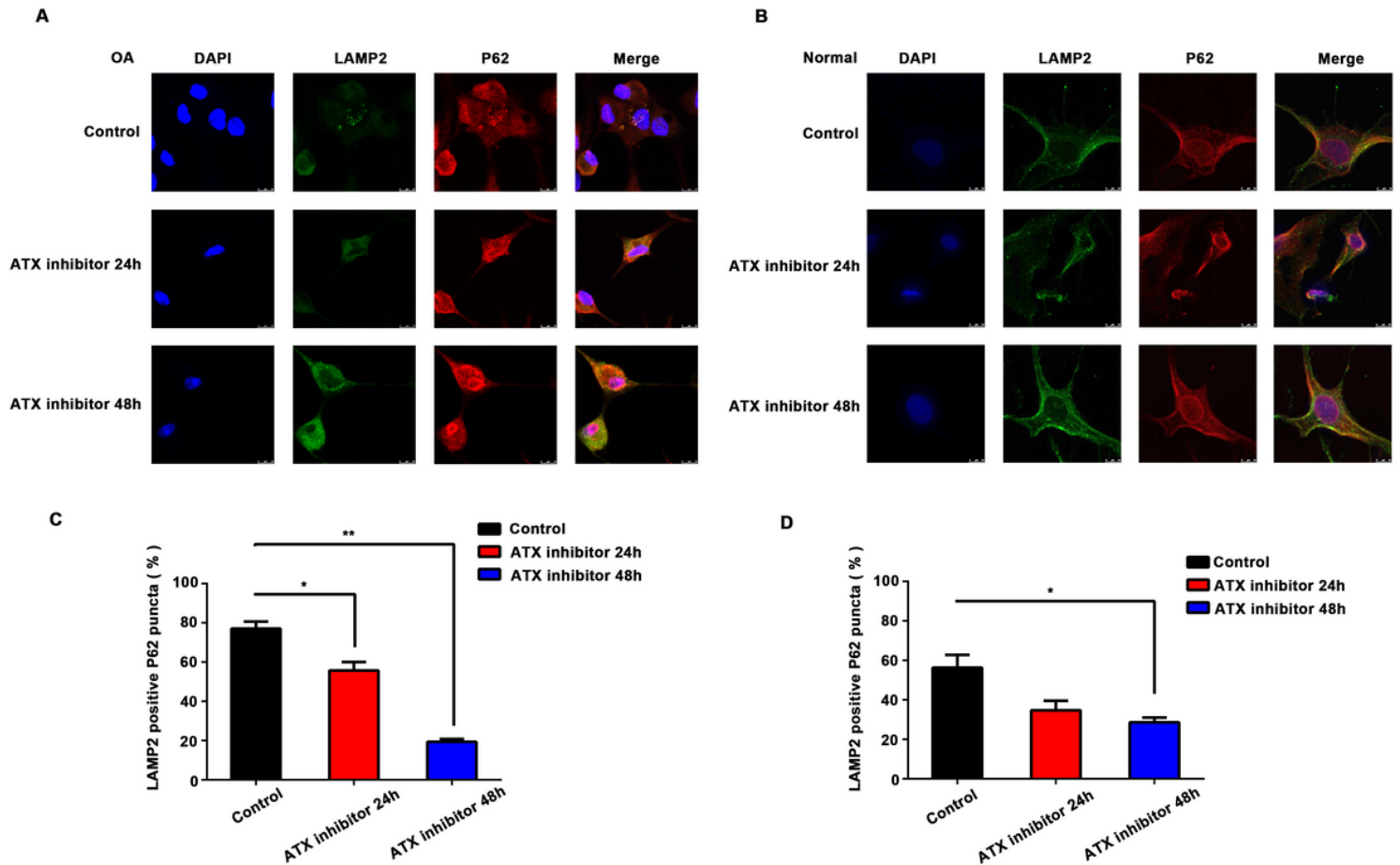


Figure 5

ATX inhibitor blocked autophagic flux by the obstruction of autophagosome and lysosome fusion. (A, B) Confocal microscopy was used to identify the localization of P62 and LAMP2. Although both the red (P62) and green (LAMP2) staining were significantly enhanced, the staining was not merged.